



**Michigan
Technological
University**

Michigan Technological University
Digital Commons @ Michigan Tech

Department of Physics Publications

Department of Physics

9-1-2008

Measurements of the vapor pressure of supercooled water using infrared spectroscopy

Will Cantrell

Michigan Technological University

Eli Ochshorn

Michigan Technological University

Alexander Kostinski

Michigan Technological University

Keith Bozin

Lawrence Technological University

Follow this and additional works at: <https://digitalcommons.mtu.edu/physics-fp>


 Part of the [Physics Commons](#)

Recommended Citation

Cantrell, W., Ochshorn, E., Kostinski, A., & Bozin, K. (2008). Measurements of the vapor pressure of supercooled water using infrared spectroscopy. *Journal of Atmospheric and Oceanic Technology*, 25(9), 1724-1729. <http://dx.doi.org/10.1175/2008/JTECHA1028.1>

Retrieved from: <https://digitalcommons.mtu.edu/physics-fp/217>

Follow this and additional works at: <https://digitalcommons.mtu.edu/physics-fp>

 Part of the [Physics Commons](#)

Measurements of the Vapor Pressure of Supercooled Water Using Infrared Spectroscopy

WILL CANTRELL, ELI OCHSHORN, AND ALEXANDER KOSTINSKI

Department of Physics, Michigan Technological University, Houghton, Michigan

KEITH BOZIN

Lawrence Technological University, Southfield, Michigan

(Manuscript received 14 May 2007, in final form 6 December 2007)

ABSTRACT

Measurements are presented of the vapor pressure of supercooled water utilizing infrared spectroscopy, which enables unambiguous verification that the authors' data correspond to the vapor pressure of liquid water, not a mixture of liquid water and ice. Values of the vapor pressure are in agreement with previous work. Below -13°C , the water film that is monitored to determine coexistence of liquid water (at one temperature) and ice (at another, higher, temperature) de-wets from the hydrophilic silicon prism employed in the authors' apparatus. The de-wetting transition indicates a quantitative change in the structure of the supercooled liquid.

1. Introduction

Below the melting point, the equilibrium vapor pressure (hereafter referred to simply as vapor pressure) of liquid water exceeds that of ice at the same temperature. Because of that difference in vapor pressure, in clouds, once any droplet freezes, it grows by condensation at the expense of surrounding droplets that have not frozen. To calculate the rate at which the mass transfer proceeds, both vapor pressures must be known as it is the difference (i.e., gradient) that drives diffusion.

The vapor pressure of ice is well established (Murphy and Koop 2005). The vapor pressure of supercooled water is less certain, principally because of difficulties inherent in measuring properties of metastable states. In this case, one must prevent the water from freezing on the time scale of the experiment. Though water can be held at slight supercoolings almost indefinitely, deeper supercoolings have short lifetimes. As a conse-

quence, most measurements of the vapor pressure are limited to temperatures higher than about -20°C .

Kraus and Greer (1984) made direct measurements of the vapor pressure of water from 0° to -22°C . Bottomley (1978) measured the difference in vapor pressures of supercooled water and ice at the same temperature, which can be used to evaluate the vapor pressure of the liquid once that of ice is known. One way to extend the temperature range is to work with smaller samples, a fact that Fukuta and Gramada (2003) utilized. By measuring the temperature difference necessary to equalize the vapor pressures of a small, supercooled droplet of water at one temperature and ice at another, higher temperature, they were able to extend their measurements to -30°C .

We present measurements of the vapor pressure of supercooled water using a similar but more sensitive method. Whereas Fukuta and Gramada monitored the equilibrium between their droplet and the ice reservoir by monitoring the size of the droplet with an optical microscope, we use a thin film of water in equilibrium with an ice reservoir. We monitor the thin film using attenuated total reflection infrared spectroscopy, which enables us to detect submonolayer changes in its thickness. Additionally, the infrared spectra ensure that we

Corresponding author address: Will Cantrell, Dept. of Physics, Michigan Technological University, 1400 Townsend Dr., Houghton, MI 49931.
E-mail: cantrell@mtu.edu

are measuring the vapor pressure of water, not a mixture of water and ice. Before describing the details of our experiment and our results, we make a brief digression into the thermodynamics of supercooled water.

2. Background on the thermodynamics of supercooled liquid water

The slope of a phase boundary on a pressure–temperature diagram is given by the Clapeyron equation:

$$\frac{dp}{dT} = \frac{\Delta s}{\Delta v}, \quad (1)$$

where Δs is the difference in the molar entropies between the two phases and Δv is the difference in the molar volumes. If the phase transition is reversible, the difference in the molar entropies can be associated with a definite amount of heat, $\Delta s = L/T$, where L is the latent heat of the phase transition at temperature T .

In the liquid–vapor transition, where the molar volume of the vapor is much greater than that of the liquid, the Clapeyron equation can be manipulated into a form known as the Clausius–Clapeyron equation:

$$\frac{dp}{dT} = \frac{L_v p}{RT^2}. \quad (2)$$

Furthermore, if the latent heat can be approximated as constant over the temperature range, Eq. (2) becomes

$$p = p_0 \exp\left[\frac{L_v}{R} \left(\frac{T - T_0}{TT_0}\right)\right], \quad (3)$$

where p_0 is the vapor pressure at a reference temperature, T_0 .

Reversibility is a key element of the argument in going from Eq. (1) to (2). The difference in the molar entropies of the two phases can only be associated with a definite quantity of heat on the equilibrium phase boundary where the transition is reversible (see, e.g., Zemansky 1957, chapter 15). In other words, latent heats involving metastable states must be examined carefully to ensure that the transition in question is, in fact, reversible. For instance, vaporization of supercooled liquid water can be done reversibly, whereas freezing of the same supercooled liquid is never reversible. (The equilibrium between the supercooled liquid and its vapor is stable. There is no equilibrium between supercooled water and ice.) The requirements of reversibility introduce a peculiar situation into measurements involving the vapor pressure of supercooled water. Such measurements are, in some sense, always probabilistic because the water may freeze. In other

words, a path connecting two states in which the supercooled water is in equilibrium with its vapor may be traversed reversibly in most instances, but there is always the probability that a fluctuation within the liquid will initiate freezing (Pruppacher and Klett 1997, chapter 7). (That probability is very low for small supercooling, but it is nonzero.)

The insistence on reversibility has the following consequence. Given the vapor pressure of water as a function of temperature (below the melting point), one might be tempted to derive L_v as a function of temperature, then use the relationship, $L_s = L_f + L_v$, where L_s is the latent heat of sublimation and L_f is the latent heat of fusion, to deduce the latent heat of fusion as a function of temperature [see, e.g., the *Smithsonian Meteorological Tables* (List 1951) and Fukuta and Gramada (2003)]. This step can be taken only when all three phase transitions may be accomplished reversibly, which occurs only at the triple point. The latent heat of fusion, L_f , is problematic for supercooled water because the system does not fulfill the requirement that the transition be reversible. Of course, freezing will involve a release of heat, but only in the case of a reversible transition can that heat be associated with the difference in the molar entropies that appears in the Clapeyron equation.

One alternative to measuring the latent heat as a function of temperature is to deduce L_v at one point on the phase boundary, then use the difference in the heat capacities of the liquid and vapor to calculate further points through Kirchoff's relation:

$$\frac{dL_v}{dT} \approx \Delta c_p(T), \quad (4)$$

where we have used the fact that the molar volume of the vapor vastly exceeds that of the liquid (see, e.g., Denbigh 1966, 200–201). The advantage of this method is that measurements of heat capacity are not constrained to a reversible path.

3. Experiment

The basis of the experiment is the difference in the chemical potential, and therefore vapor pressure, between a stable and metastable phase at the same temperature. That, coupled with Ostwald's rule of stages, allows us to use the vapor pressure of ice at a given temperature to infer the vapor pressure of supercooled water at another, lower temperature. Our setup is similar in spirit to the one that Fukuta and Gramada (2003) used.

A schematic is shown in Fig. 1. The prism housing and chamber are essentially the same as those de-

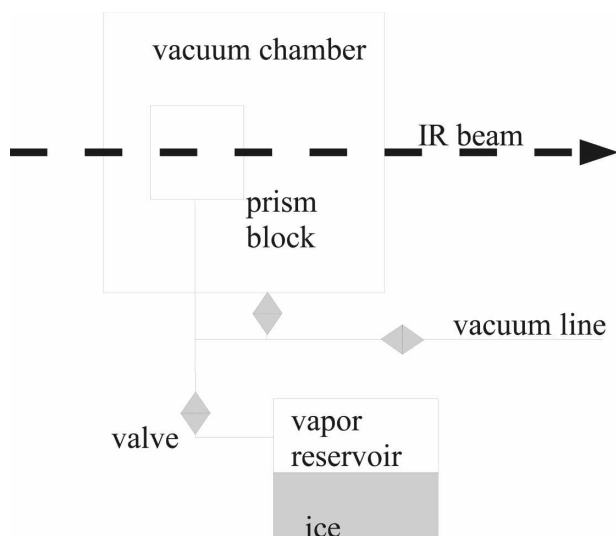


FIG. 1. A schematic of the setup of the vapor reservoir and the chamber that houses the prism.

scribed in Ochshorn and Cantrell (2006). Briefly, the infrared beam is directed out of the spectrometer (Bruker, Tensor 37). It is reflected off a gold-coated, parabolic mirror (Janos Technology) into the chamber shown in Fig. 1. Upon exiting the chamber, the beam is focused onto a liquid-nitrogen-cooled mercury-cadmium-telluride (MCT) detector (Bruker) with a gold-coated elliptical mirror (Bruker).

The prism (Reflex Analytical) is silicon, treated to make it hydrophilic. It is housed in an aluminum block (drilled through for optical access), which is seated on a Peltier cooler. The temperature of the prism is monitored with a thin-film resistance thermometer (RTD; Minco), which is affixed to the aluminum block. We calibrate for the spatial separation between the working surface of the prism and the temperature sensor by melting a microliter drop of water on the prism with a ramp rate of 0.02 K min^{-1} . The point at which the spectra show the ice-to-water transition is the melting point. Using this calibration, we have a temperature uncertainty for the prism of 0.1°C . The prism is held under vacuum for approximately 30 min at room temperature after it is cleaned and before water vapor is introduced into the chamber. This ensures that residual water from cleaning evaporates. (The spectra show no water on the surface before it is leaked into the chamber.) The prism and its housing are in a chamber, which is evacuated to less than 10^{-3} mbar.

The vapor reservoir is frozen spectrophotometric-grade water (Alfa Aesar). Its temperature is monitored with a tip-sensitive RTD (Minco) that protrudes through the wall of the chamber near the ice-vapor

interface. The reservoir is thermostatted with a Lakeshore temperature controller (Model 331); the uncertainty in the temperature of the reservoir is $\pm 0.1^\circ\text{C}$. The line connecting the reservoir and prism is evacuated before each experiment. The only gas present in the system in appreciable quantities is water vapor.

We begin an experiment with the temperature of the prism 1° or 2° greater than the vapor reservoir. Using a thermoelectric temperature controller (Melcor), we lower the temperature of the prism in increments of 1° to $\frac{1}{2}^\circ$, while monitoring the absorbance spectra. At each step, the system is allowed to equilibrate. [Equilibration is based on the magnitude of the change in the absorbance spectra (see below).] When the vapor pressure of water drops below that of ice, liquid water begins to condense on the prism, which is apparent in the spectra. The temperature at which water begins to condense on the prism is assigned to the vapor pressure of supercooled water at that temperature. The vapor pressure is calculated from the vapor pressure of ice at the higher temperature, using Eq. (7) in Murphy and Koop (2005):

$$p_{\text{ice}} = \exp(9.550426 - 5723.265/T + 3.53068 \ln(T) - 0.00728332T), \quad (5)$$

where p_{ice} is in pascals and T is in kelvins. The equation is valid for $T > 110 \text{ K}$.

One advantage to using infrared spectroscopy in this way is that the phase of the film condensed on the prism can be monitored. As noted above, when first exposed to water vapor, the temperature of the prism is 1° or 2° higher than the temperature of the ice in the reservoir. Water sticks to the prism (and is apparent in the spectra), but it is adsorbed. This interfacial water is neither liquid nor ice. It is simply the water that sticks to a given surface for a given relative humidity. However, at some point, as the temperature of the prism decreases, the vapor pressure of water drops below that of ice at the higher temperature, resulting in a net flux of vapor to the prism and condensation of the liquid. The infrared spectra show that it is, in fact, liquid on the prism, not ice.

The difference between liquid and ice can be seen in Fig. 2, which is a plot of the absorption bands of 15-nm films of water and ice on a silicon prism. [As the magnitude of the spectra in Fig. 3 (left) shows, the liquid water films we monitor are of order 15 nm.] The peak position differs by $\sim 200 \text{ cm}^{-1}$. The ice band is narrower and ice has a bigger absorption cross section. In our measurements, the consistency of the peak position and band shape show that the water does not freeze. A nucleation event would propagate through the film in less than a second, leaving only ice.

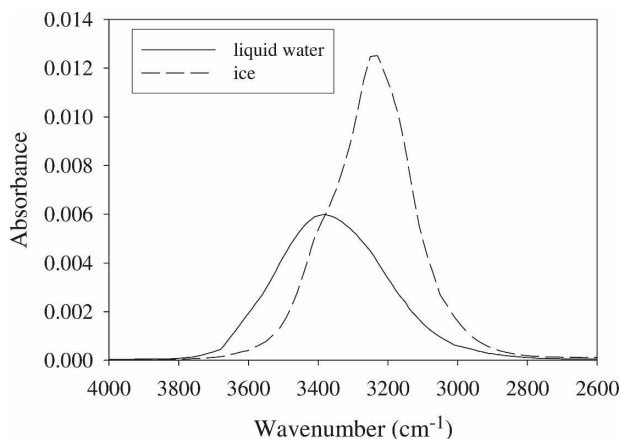


FIG. 2. Calculated spectra of 15-nm-thick water and ice films on a silicon prism. Upon freezing, the peak in the absorbance band shifts from ~ 3400 to 3200 cm^{-1} , and the band narrows. The differences in the position of the peak, width of the band, and magnitude, which are apparent in this figure, allow us to verify that the water on the prism does not freeze during the experiment. The spectra are calculated using optical constants from Downing and Williams (1975) and Clapp et al. (1995).

4. Results

Spectra from a typical experiment and the corresponding integrated absorbances are shown in Fig. 3. The left-hand panel shows five separate groupings of spectra, four of which correspond to an equilibrium between the vapor and water adsorbed to the prism. That equilibrium indicates that the chemical potential of the liquid at the temperature of the prism still exceeds the chemical potential of ice. The last set of spectra (greatest magnitudes in the figure) corresponds to

the case where the chemical potential of the liquid falls below that of ice. The imbalance results in a net flux of vapor to the prism and condensation of liquid. (Note that the peak position is 3400 cm^{-1} , indicative of the liquid, not ice.)

For this particular experiment, the integrated absorbance (Fig. 3, right) shows equilibrium between ice at -7°C and water adsorbed to the prism for all temperatures greater than -9°C at the prism. Again, the steady growth apparent at -9°C indicates that the chemical potential of liquid water has dropped below that of ice. There is a pair of temperatures such that the chemical potentials of ice and supercooled water are equal. The vapor pressure of water can then be calculated from the temperature of the ice reservoir using Eq. (5).

Our vapor pressures are shown in Fig. 4. They are consistent with those of previous investigators over the temperature range accessible to us (see below). In particular we note that our measurements corroborate the work by Fukuta and Gramada (2003), which has been criticized for its apparent disagreement with the molar heat capacity of water (Murphy and Koop 2005). We believe that Fukuta and Gramada's vapor pressure measurements are not in error but that the discrepancy lies in the application of Kirchoff's equation [Eq. (4)] to derive the latent heat of fusion, L_f . Fukuta and Gramada (2003) derive L_f using the relationship between the latent heats at the triple point (see section 2). That relationship is valid *only* at the triple point, where all three phase changes are reversible, so it cannot be used to derive L_f as a function of T . [The notion of L_f below the melting point is subtle in any case; see Kostinski and Cantrell (2008).]

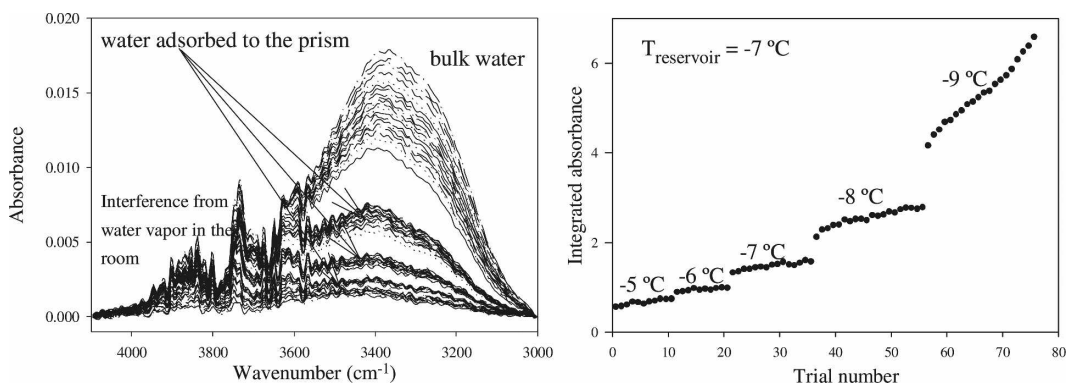


FIG. 3. (left) A series of spectra from a typical experiment. The jagged features at wavenumbers greater than 3600 cm^{-1} are from residual water vapor in the purge box. The time between successive spectra at a given temperature is 60 s. When the temperature of the prism is changed, the system is allowed to equilibrate for several minutes before measurements resume. (right) Integrated absorbance of the liquid water band ($3050\text{--}3600\text{ cm}^{-1}$) corresponding to the spectra in the left-hand figure. The temperature of the reservoir is -7°C ; the temperature of the prism at each stage is shown next to the corresponding data points. At each temperature greater than -9°C , the absorbance signal stabilizes, indicating water adsorbed to the prism. At -9°C the vapor pressure of liquid water at the prism falls below that of ice at -7°C , resulting in condensation of the liquid on the prism.

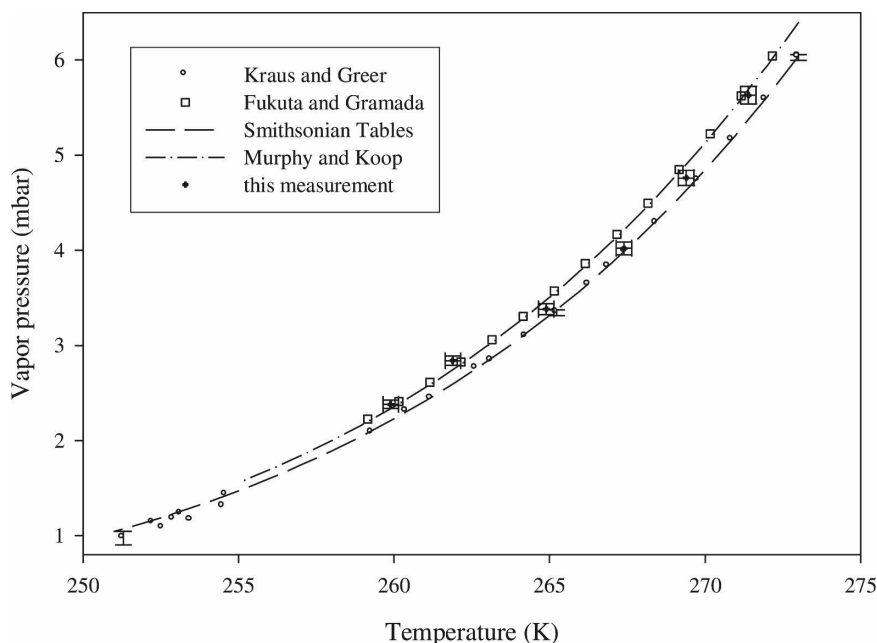


FIG. 4. Vapor pressure of supercooled water as a function of temperature from Kraus and Greer (1984), Fukuta and Gramada (2003), and this measurement, along with formulations from Murphy and Koop (2005) and the *Smithsonian Meteorological Tables* (List 1951). For our data, the error bar in temperature corresponds to the difference between the temperature of the prism at which water was simply adsorbed and that where the liquid began to condense. The error bar in pressure corresponds to the uncertainty in the temperature of the vapor reservoir, which translates to an uncertainty in the vapor pressure of ice.

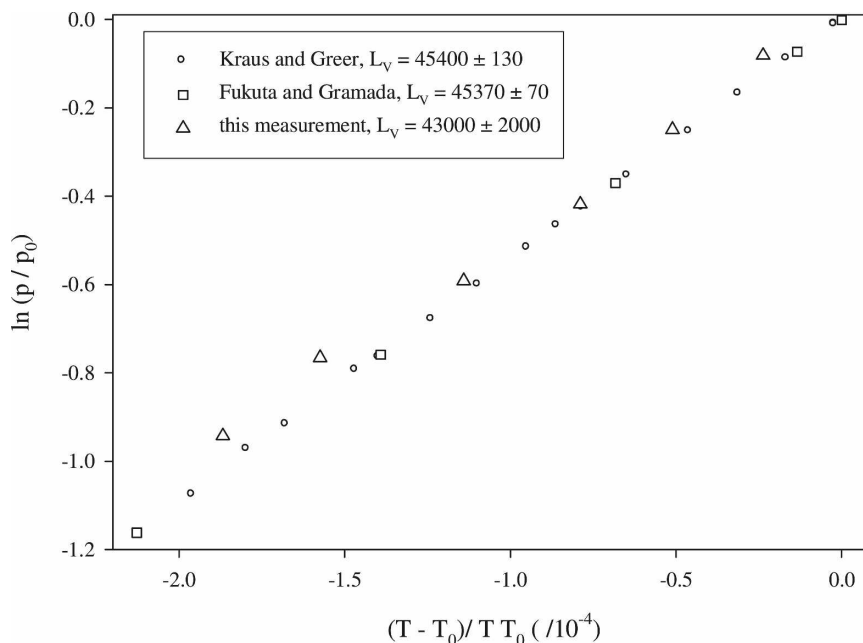


FIG. 5. A plot of $\ln(p/p_0)$ vs $(T - T_0)/TT_0$ for three of the datasets discussed here. The slope of the line is \bar{L}_v/R . The corresponding value of \bar{L}_v (in J mol^{-1}) is given in the legend to the figure. The quoted uncertainties are derived from the uncertainty of the fit to the data shown in the figure. Here $p_0 = 6.1078$ mb at $T_0 = 0^\circ\text{C}$.

Figure 5 is a plot of $\ln(p/p_0)$ versus $(T - T_0)/TT_0$ for the three datasets taken most directly from measurements. The slope of the best-fit line to the data is \bar{L}_v/R . All three values are within 7% of the value derived from Murphy and Koop [2005, their Eq. (9)], $45\,600 \pm 300 \text{ J mol}^{-1}$.

5. Discussion

Our measurements of the vapor pressure of supercooled water are in agreement with previous work—measured (Kraus and Greer 1984; Fukuta and Gramada 2003), extrapolated from higher temperature measurements (the *Smithsonian Meteorological Tables*), and derived from thermodynamic relations using other properties of water (Murphy and Koop 2005). Our initial goal was to measure the vapor pressure for deeply supercooled water (approaching -30°C) as Fukuta and Gramada (2003) did. We were unable to accomplish that goal because of water's peculiar behavior at low temperatures. Though we can reliably supercool water well past -20°C on our prism, the films are morphologically unstable. For temperatures less than -13°C , the water film de-wets from the prism. The abrupt departure from a plane-parallel interface makes reliable interpretation of the infrared spectra in our attenuated total reflection setup impossible. The dewetting transition indicates a change in the structure of the liquid and its interaction with the substrate, which is interesting in its own right (and relevant for nucleation studies) but is not germane to the discussion here.

Because measurements of the vapor pressure are assumed to occur reversibly, they satisfy the condition for identifying a difference in the molar entropies of the phases with heat. Therefore, vapor pressure measurements can be used to determine the latent heat of vaporization as we did above. They cannot, however, be subtracted from the latent heat of sublimation to derive the latent heat of fusion below the melting point. As discussed in section 2, that relation is valid only at the triple point, where all three phase transitions occur reversibly. Fukuta and Gramada's measurements have been criticized for an apparent discrepancy with measured values of the heat capacity of liquid water. This is only an apparent discrepancy. The latent heat of fusion below the melting point cannot be derived from values of the vapor pressure of the liquid, and Kirchoff's relation [Eq. (4)] cannot be applied to liquid-crystal transitions below the melting point because it is valid only on the equilibrium phase boundary.

6. Conclusions

We have presented measurements of the vapor pressure of water from the melting point to -13°C . Our values are in agreement with previous work, both measured and based on thermodynamic relations with other measured properties of water. For temperatures below -13°C , the film of water on the silicon prism in our system de-wets, making measurements at lower temperatures impossible. However, from the melting point down to -13°C , we have verified that it is the vapor pressure of the liquid we are measuring; the infrared spectra provide an unambiguous verification of the phase of the condensate.

Acknowledgments. Funding from NASA's New Investigator Program and from the National Science Foundation (ATM01-06271, ATM05-54670, and CHE-0410007) is appreciated. Portions of this paper derive from work done while AK was at the Weizmann Institute of Science in Rehovot, Israel, as a Weston visiting professor, and he is grateful to the Physics of Complex Systems Division and to Gregory Falkovich for their hospitality and support. Thanks also to Raymond Shaw for lending us the temperature controller.

REFERENCES

- Bottomley, G., 1978: Vapor-pressure of supercooled water and heavy-water. *Austr. J. Phys.*, **31**, 1177–1180.
- Clapp, M., R. Miller, and D. Worsnop, 1995: Frequency-dependent optical constants of water ice obtained directly from aerosol spectra. *J. Phys. Chem.*, **99**, 6317–6326.
- Denbigh, K., 1966: *The Principles of Chemical Equilibrium: With Applications in Chemistry and Chemical Engineering*. 2nd ed. Cambridge University Press, 494 pp.
- Downing, H., and D. Williams, 1975: Optical constants of water in the infrared. *J. Geophys. Res.*, **80**, 1656–1661.
- Fukuta, N., and C. Gramada, 2003: Vapor pressure measurement of supercooled water. *J. Atmos. Sci.*, **60**, 1871–1875.
- Kostinski, A., and W. Cantrell, 2008: Entropic aspects of supercooled droplet freezing. *J. Atmos. Sci.*, **65**, 2961–2971.
- Kraus, G., and S. Greer, 1984: Vapor pressures of supercooled water and deuterium oxide. *J. Phys. Chem.*, **88**, 4781–4785.
- List, R., Ed., 1951: *Smithsonian Meteorological Tables*. 6th ed. Smithsonian Institution, 527 pp.
- Murphy, D., and T. Koop, 2005: Review of the vapour pressures of ice and supercooled water for atmospheric applications. *Quart. J. Roy. Meteor. Soc.*, **131**, 1539–1565.
- Ochshorn, E., and W. Cantrell, 2006: Towards understanding ice nucleation by long chain alcohols. *J. Chem. Phys.*, **124**, 054 714.
- Pruppacher, H., and J. Klett, 1997: *Microphysics of Clouds and Precipitation*. 2nd ed. Kluwer Academic, 954 pp.
- Zemansky, M., 1957: *Heat and Thermodynamics*. 4th ed. McGraw-Hill, 484 pp.

CORRIGENDUM

WILL CANTRELL, ELI OCHSHORN, AND ALEXANDER KOSTINSKI

Department of Physics, Michigan Technological University, Houghton, Michigan

KEITH BOZIN

Lawrence Technological University, Southfield, Michigan

Due to an error, vapor pressure data from Murphy and Koop (2005) and Fukuta and Gramada (2003) were plotted incorrectly in Fig. 4 in Cantrell et al. (2008). The correct version of Fig. 4 is presented below. (Note that the vapor pressure data we are reporting are unchanged.)

REFERENCES

- Cantrell, W., E. Ochshorn, A. Kostinski, and K. Bozin, 2008: Measurements of the vapor pressure of supercooled water using infrared spectroscopy. *J. Atmos. Oceanic Technol.*, **25**, 1724–1729.
- Fukuta, N., and C. Gramada, 2003: Vapor pressure measurement of supercooled water. *J. Atmos. Sci.*, **60**, 1871–1875.
- Kraus, G., and S. Greer, 1984: Vapor pressures of supercooled H₂O and D₂O. *J. Phys. Chem.*, **88**, 4781–4785.
- List, R., Ed., 1951: *Smithsonian Meteorological Tables*. 6th ed. Smithsonian Institution, 527 pp.
- Murphy, D., and T. Koop, 2005: Review of the vapour pressures of ice and supercooled water for atmospheric applications. *Quart. J. Roy. Meteor. Soc.*, **131**, 1539–1565.

Corresponding author address: Will Cantrell, Dept. of Physics, Michigan Technological University, 1400 Townsend Dr., Houghton, MI 49931.
E-mail: cantrell@mtu.edu

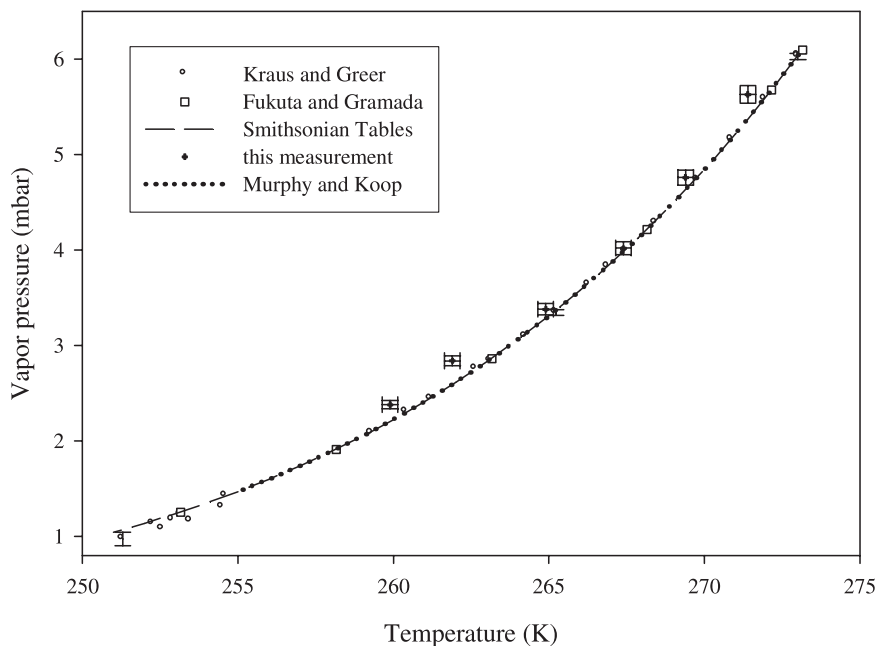


FIG. 4. Vapor pressure of supercooled water as a function of temperature from Kraus and Greer (1984), Fukuta and Gramada (2003), and this measurement, along with formulations from Murphy and Koop (2005) and the *Smithsonian Meteorological Tables* (List 1951). For our data, the error bar in temperature corresponds to the difference between the temperature of the prism at which water was simply adsorbed and that where the liquid began to condense. The error bar in pressure corresponds to the uncertainty in the temperature of the vapor reservoir, which translates to an uncertainty in the vapor pressure of ice.